ACS APPLIED MATERIALS & INTERFACES

Research Article

www.acsami.org

3D Graphene Foam as a Monolithic and Macroporous Carbon Electrode for Electrochemical Sensing

Xiaochen Dong,[†] Xuewan Wang,[‡] Lianhui Wang,[†] Hao Song,[‡] Hua Zhang,[§] Wei Huang,[†] and Peng Chen*[,‡]

[†]Key Laboratory for Organic Electronics & Information Displays, Institute of Advanced Materials, Nanjing University of Posts and Telecommunications, 9 Wenyuan Road, Nanjing, 210046, China

[‡]Division of Bioengineering, School of Chemical and Biomedical Engineering, Nanyang Technological University, 70 Nanyang Drive, 637457, Singapore

[§]School of Materials Science and Engineering, Nanyang Technological University, 50 Nanyang Avenue, 639798, Singapore

Supporting Information

ABSTRACT: Graphene, a single-atom-thick monolayer of sp^2 carbon atoms perfectly arranged in a honeycomb lattice, is an emerging sensing material because of its extraordinary properties, such as exceptionally high specific surface area, electrical conductivity, and electrochemical potential window. In this study, we demonstrate that three-dimensional (3D), macroporous, highly conductive, and monolithic graphene foam synthesized by chemical vapor deposition represents a novel architecture for electrochemical electrodes. Being employed as an electrochemical sensor for detection of dopamine, 3D graphene electrode exhibits remarkable sensitivity (619.6 μA mM^{-1} cm^{-2}) and lower detection limit (25 nM at a signal-to-noise ratio of 5.6), with linear response up to ~25 μM. And the oxidation peak of dopamine can be easily distinguished from that of uric acid − a common interferent to dopamine detection. We envision that the graphene foam provides a promising platform for the development of electrochemical sensors as well as other applications, such as energy storage and conversion.

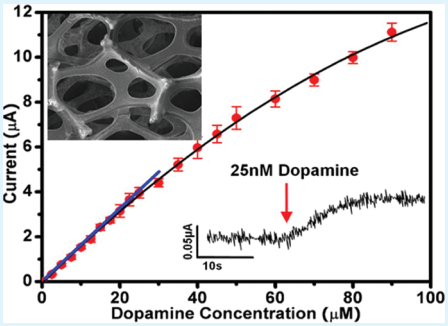

KEYWORDS: *graphene, 3D electrode, electrochemical detection, dopamine, sensors, nanomaterials*

INTRODUCTION

Graphene, a single-atom-thick monolayer of sp^2 carbon atoms perfectly arranged in a honeycomb lattice, is an emerging sensing material because of its extraordinary structural, electrical, optical, and mechanical properties.[1−6] In particular, this new carbonaceous material, which exhibits large specific surface area, high charge carrier capacity and mobility, and unique electrochemical properties, has recently attracted tremendous interest to be employed as the electrode material in various novel electrochemical sensors.[7−11] In most of the current developments, graphene derivative (reduced graphene oxide, rGO) is used, sometimes hybridizing with other functional materials, to coat the conventional electrode (e.g., glassy carbon electrode).[12−14]

Conventionally, the electrochemical electrode is planar. Therefore, the active surface area is limited. To tackle this problem, nanostructure materials (e.g., carbon nanotube) are used to coat the flat electrode surface in order to increase the specific surface area, thus, sensitivity of detection.[15−17] However, such surface expansion is still inherently limited by the two-dimensional (2D) nature of the planar electrodes. Some attempts have thus been made to construct three-dimensional (3D) electrodes. For example, electrochemical electrode based 3D polymeric matrix with embedded enzymes and gold nanoparticles has been developed to detect lactic acid.[18] However, nanoporous composites of such kind are not adequately efficient in charge transfer and mass transport. And their architecture and morphology cannot be precisely controlled. Alternatively, photolithographic microfabrication has been used to make 3D electrode with regular array of standing nanopillars.[19] But this method involves sophisticated lithographic techniques in a clean room.

In the present work, we demonstrate the use of chemical vapor deposition (CVD) grown three-dimensional (3D) graphene foam[20,21] as a novel free-standing and monolithic electrochemical electrode. With large specific surface area, 3D multiplexed and highly conductive pathways, and well-defined macroporous structure, this new electrode architecture holds great promise for various electrochemical sensing. To demonstrate its potential, we used it here for the detection of dopamine. Dopamine is a critical neurotransmitter, deficiency of which leads to various neurological diseases, such as Parkinson's disease.

Received: March 14, 2012
Accepted: May 11, 2012
Published: May 11, 2012

 © 2012 American Chemical Society

EXPERIMENTAL SECTION

Fabrication of Freestanding Graphene Foam Electrodes. As described previously,[22,23] 3D graphene foam was synthesized by chemical vapor deposition under atmospheric pressure, with nickel foam as the growth substrate and ethanol as the precursor.[24,25] After growth, the nickel substrate was removed by 3 M HCl at 80 °C overnight. The freestanding of 3D graphene foam (0.5 cm × 0.5 cm, 1 mm thick) was then fixed onto a glass slide, and an electrical lead was made by silver paint and insulated with silicone rubber (shown in Figure 1a).

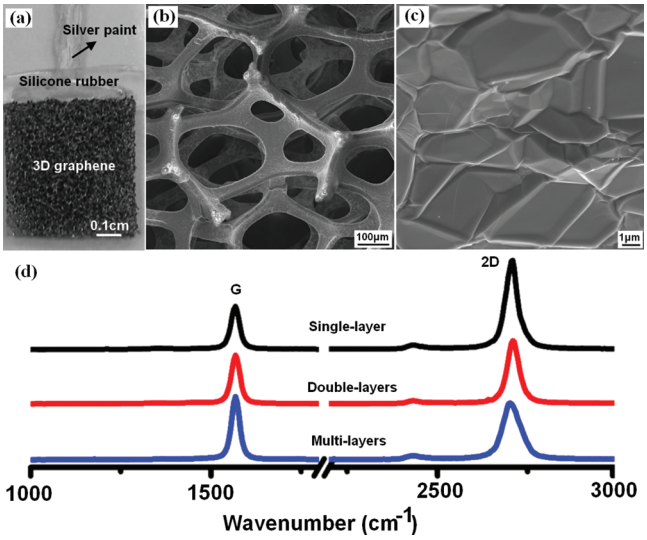

Figure 1. (a) Optical image of a 3D graphene electrode. (b, c) SEM images of 3D graphene foam at different magnification. (d) Raman spectra of 3D graphene foam obtained at different positions.

Characterizations. The morphology of 3D graphene foam was observed by a scanning electron microscopy (SEM, JEOL, JSM-6700F). The Raman spectra (excited at 488 nm) were obtained by a confocal Raman microscope (CRM200, WITec). The specific surface area of 3D graphene foam was determined by measuring nitrogen adsorption−desorption isotherms at 77 K using a Quantachrome NOVA-3000 system.

Electrochemical Measurements. All electrochemical measurements were carried out with a three-electrode system (CHI660D electrochemical workstation, Chenhua, China) using 0.1 M phosphate buffer solution (PBS, PH 7.2) as the electrolyte. The 3D graphene foam was used as the working electrode. Ag/AgCl electrode and platinum plate were used as the reference electrode and counter electrode, respectively. Dopamine and uric acid were purchased from Sigma-Aldrich and used without any further purification.

RESULTS AND DISCUSSION

The morphology of the 3D graphene foam is characterized by SEM. As shown in Figure 1b, graphene foam exhibits well-defined macroporous structure with the pore diameter ∼100−200 μm. And it offers a large specific surface area (∼670 m^2/g as determined by Brunauer−Emmett−Teller N_2 adsorption−desorption). The thin graphene scaffold has a smooth surface, assuming the identical surface topology as nickel substrate due to conformal CVD growth (Figure 1c). The Raman spectra of 3D graphene foam obtained at different positions is demonstrated in Figure 1d. As shown, the Raman spectra present two prominent characteristic peaks at ∼1560 and ∼2700 cm^{-1}, corresponding to the G and 2D band of graphene, respectively.[26] The intensity ratio of G and 2D band indicates that the graphene foam is composed of single and few layer graphene domains.[27] In addition, the absence of D band at ∼1350 cm^{-1} suggests that the resulting graphene foam is of high quality (i.e., no defects), ensuring high electrical conductivity as compared with the commonly used reduced graphene oxide sheets. Due to the excellent mechanical strength of graphene, graphene foam remains free-standing after etching away the underlying nickel foam despite its atomistic thin scaffold. Although not visible under SEM, nickel impurities, however, are left on graphene foam as revealed by energy-dispersive X-ray spectroscopy (EDX) (see Figure S1 in the Supporting Information). On the other hand, the nickel impurities may be beneficial to enhance the electrocatalytic activities of graphene electrodes.[28]

To compare the electrochemical performance of 3D graphene electrode with the conventional planar glassy carbon (GC) electrode, their cyclic voltammograms (CV) measured in the phosate buffer solution (PBS: 0.1 M, pH 7.2) containing 5.0 mM $K_3[Fe(CN)_6]$ is shown in Figure 2a. The electrochemical signal from the 3D graphene electrode is several-folds larger than that from GC electrode. As $K_3[Fe(CN)_6]$ is a commonly used mediator in various electrochemical sensors, this observation suggests the potential of 3D graphene foam

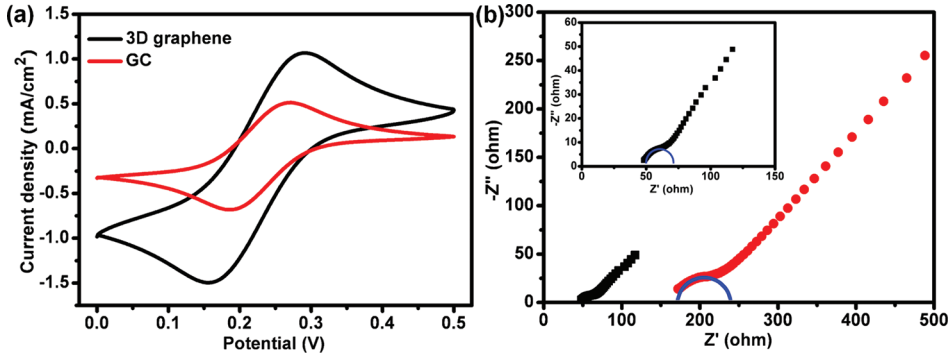

Figure 2. (a) Cyclic voltammograms of glassy carbon (GC) electrode and 3D graphene foam electrode at a scan rate of 20 mV/s in PBS solution containing 5.0 mM $K_3[Fe(CN)_6]$. (b) Electrochemical impedance spectroscopy (EIS) Nyquist plots obtained from GC and graphene foam electrodes (frequency ranges from 1 Hz to 100 kHz at open-circuit potential and with a perturbation signal of 5 mV). The inset shows the enlarged plot of 3D graphene electrode. The preceding portion of the Nyquist plot is fitted with a semicircle.

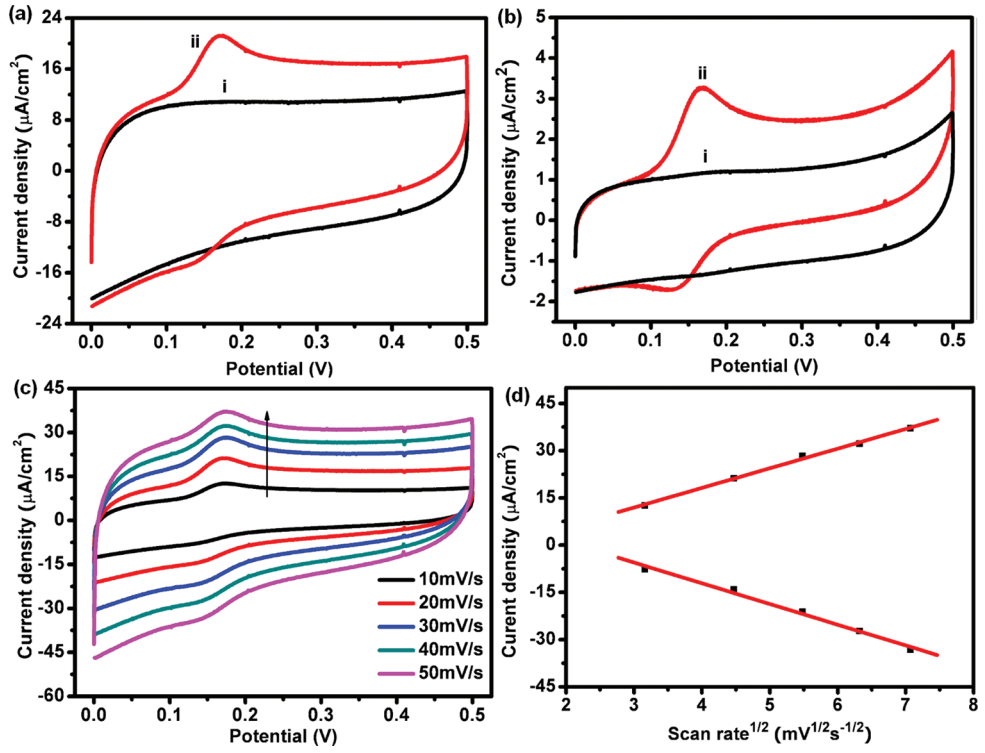

Figure 3. CV plots of 3D graphene electrode (a) and glassy carbon electrode (b) in PBS (i) without and (ii) with 20 μM dopamine. Scan rate = 20 mV/s. (c) CV plots of the 3D graphene foam electrode in 20 μM dopamine solution (0.1 M PBS, PH 7.2) at different scan rates: 10, 20, 30, 40, and 50 mV/s. The arrow indicates the increase direction of scan rate. (d) The anodic peak current (top) or catholic peak current (bottom) vs square root of the scan rate.

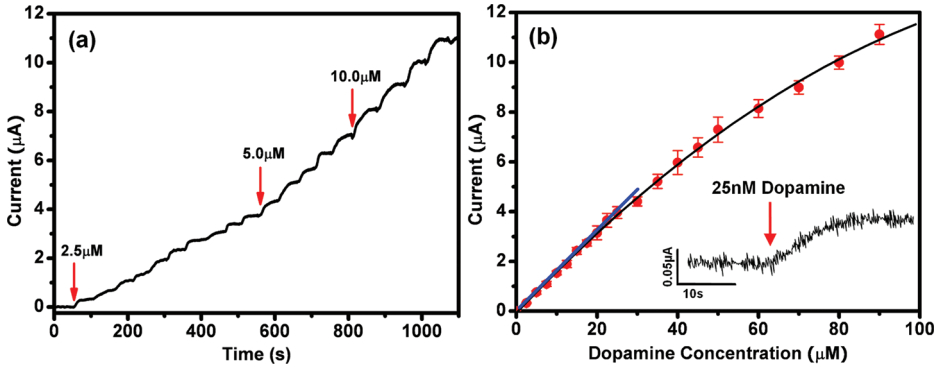

Figure 4. (a) Amperometric response (at 0.177 V) of the freestanding 3D graphene foam electrode upon addition of dopamine to PBS solution. The background current is subtracted. (b) The average dose−response curve from three electrodes. The error bars indicate the standard deviations. A linear fitting is shown at low concentration range. And the inset shows the amperometric response to 25 nM dopamine.

electrode for highly sensitive electrochemical detection. Furthermore, it is noted that the potential separation between the anodic and cathodic peaks ($\Delta E_p \approx 0.132$ V) of 3D graphene electrode is larger than that of GC electrode ($\Delta E_p \approx$ 0.08 V), indicating that the 3D graphene foam electrode has a much higher charge transfer rate. Electrochemical impedance spectroscopy (EIS) was used to determine the charge-transfer resistance as indicated by the diameter of the preceding semicircle in Nyquist plot (Figure 2b).[29] It is found that the charge transfer resistance of 3D graphene foam (~20.7 Ω) is significantly smaller than that of 2D GC electrode (~69 Ω). This is because of the high electrical conductivity of graphene and the vastly multiplexed conductive pathways provided by the 3D graphene. These experiments demonstrate the superior performance of 3D graphene for electrochemical detection.

Next, we used the 3D graphene electrode to detect dopamine - a critical neurotranmitter in the central nervous system. As shown in panels a and b in Figure 3, in the presence of 20 μM dopamine, the CVs of both 3D graphene electrode and GC electrode display a pair of redox peaks. But note that the magnitude of CV response from the 3D graphene foam is much greater. And the peak-to-peak potential sepration from the 3D graphene foam is also larger than the GC electrode (0.046 V vs 0.033 V), suggesting a faster charge transfer rate. Furthermore, panels c and d in Figure 3 demonstrate that both cathodic and anodic peak currents from the 3D graphene electrode linearly scale with the square root of scan rate, indicating that the electrochemical reaction is a reversible and diffusion-controlled electrochemical process.[30] Furthermore, degradation in electrode responses is not observed after repetitive CV scanning,

dx.doi.org/10.1021/am300459m | ACS Appl. Mater. Interfaces 2012, 4, 3129−3133

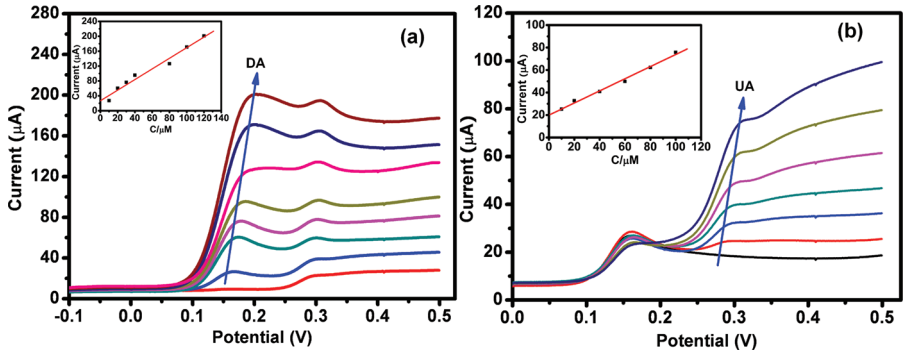

Figure 5. Linear sweep voltammogram (LSV) plots of the 3D graphene electrode in PBS solution containing, (a) 40 μM uric acid (UA) with different concentrations of dopamine (DA): 0, 10, 20, 30, 40, 80, 100, and 120 uM; or (b) 10 μM DA with different concentrations of UA: 0, 10, 20, 40, 60, 80, 100uM. Scan rate = 50 mV/s. The inset shows the relation of peak oxidative current to DA (or UA) concentration.

indicating that our electrode is not vunlerable to fouling. In agreement with the previous report,[31] we also observed pH dependence of dopamine oxidation. As shown in Figure S2 (see the Supporting Information), the maximum redox current is obatined at pH 5.5 while no redox peaks are observed at high pH. This is because the hydroxyl groups of dopamine whose deprotonation facilitates dopamine oxidation are already deprotonated in alkali media. However, as shown in Figure 3, dopamine can be sensitively detected at physiological pH.

A typical amperometric response (at +0.177 V) of the 3D graphene electrode to the addition of different concentrations of dopamine to PBS solution is shown in Figure 4a. The response to dopamine is sensitive and rapid. The average dose response (amperometric response vs dopamine concentration) (Figure 4b) demonstrates that the detection can be made within a large concentration range, and in the linear response range (up to 25 μM) an exceptional sensitivity of 619.6 μA mM^{-1} cm^{-2} is achieved. And remarkably, an obvious amperometric current (signal-to-noise ratio = 5.6) can be triggered by dopamine at a concentration as low as 25 nM (Figure 4b, inset). Notably, the performance of our 3D graphene electrode apparently outperforms the previously reported graphene modified or carbon nanotube modified planar electrodes (see Table S1 in the Supporting Information).[32,33]

Uric acid, which also exists in the extracellular fluid of the central nervous system and has similar electrochemical properties as dopamine, complicates the identification of dopamine. Therefore, we examined whether the 3D grapehene electrode is able to electrochemically distinguish uric acid and dopamine. Figure 5 shows the linear sweep voltammogram (LSV) of the 3D graphene foam electrode in the presence of both dopamine and uric acid. As seen, the oxidative peaks of dopamine and uric acid are well separated. And in the presence (interference) of uric acid (or dopamine), the peak current of dopamine (or uric acid) increases linearly with increasing concentration. These experiments suggest that dopamine and uric acid can be selectively detected. The ability of the 3D graphene electrode to distinguish dopamine and uric acid is conceivably because of the unique electronic structure of graphene and the facilitated electron transfer between dopamine and graphene as a result of their strong $\pi-\pi$ interaction.

CONCLUSIONS

In this study, we demonstrate the use of 3D graphene foam as novel electrode architecture for electrochemical sensing. As an example, we show that the 3D graphene foam can selectively detect dopamine with remarkable sensitivity and lower detection limit. Such excellent performance can be attributable to (1) large surface (active) area of 3D graphene; (2) high charge transfer rate ensured by the exceptionally high conductivity of graphene and 3D multiplexed conductive pathways of graphene foam; (3) the macroporous structure of graphene foam which ensures efficient mass transport of the diffusional redox species; and (4) the intimate interactions (hydrophobic and $\pi-\pi$ interactions) between dopamine molecules and graphene promotes electron transfer from dopamine. The 3D graphene promises a wide range of sensing applications because it can be readily functionalized or hybridized with other organic (e.g., enzymes) or inorganic materials with large capacity and it has a large electrochemical potential window[34] to enable detection of molecules with high oxidation or reduction potential.

ASSOCIATED CONTENT

Supporting Information

EDX spectrum of 3D graphene and cyclic voltammograms of 3D graphene electrode in the presence of 20 μM dopamine at different pH values. This material is available free of charge via the Internet at http://pubs.acs.org.

AUTHOR INFORMATION

Corresponding Author

*E-mail: chenpeng@ntu.edu.sg.

Notes

The authors declare no competing financial interest.

ACKNOWLEDGMENTS

We acknowledge the financial support from NNSF of China (50902071, 61076067, BZ2010043), the National Basic Research Program of China (2009CB930601, 2012CB933301), the Ministry of Education of China (IRT1148), Jiangsu Province Science Foundation for Six Great Talent Peak (RLD201103), Key Project of Chinese Ministry of Education (212058), National Research Foundation of Singapore (CRP grant: NRF-CRP-07-2), Ministry of Singapore (AcRF tier 2 grants: MOE2011-T2-2-010, MOE2010-T2-1-060), Singapore National Research Founda-

tion (CREATE programme: Nanomaterials for Energy and Water Management).

REFERENCES

(1) Liu, Y. X.; Dong, X. C.; Chen, P. *Chem. Soc. Rev.* **2012**, *41*, 2283−2307.
(2) Eda, G.; Chhowalla, M. *Adv. Mater.* **2010**, *22*, 2392−2415.
(3) Huang, Y. X.; Dong, X. C.; Liu, Y. X.; Li, L. J.; Chen, P. *J. Mater. Chem.* **2011**, *21*, 12358−12362.
(4) Che, J. F.; Shen, L. Y.; Xiao, Y. H. *J. Mater. Chem.* **2010**, *20*, 1722−1727.
(5) Dong, X. C.; Huang, W.; Chen, P. *Nanoscale Res. Lett.* **2011**, *6*, 60.
(6) Sudibya, H. G.; He, Q. Y.; Zhang, H.; Chen., P. *ACS Nano* **2011**, *5*, 1990−1994.
(7) Lu, Q.; Dong, X. C.; Li, L. J.; Hu, X. *Talanta* **2010**, *82*, 1344−1348.
(8) Ping, J. F.; Wang, Y. X.; Fan, K.; Wu, J.; Ying, Y. B. *Biosens. Bioelectron.* **2011**, *28*, 204−209.
(9) Kuila, T.; Bose, S.; Khanra, P.; Mishra, A. K.; Kim, N. H.; Lee, J. H. *Biosens. Bioelectron.* **2011**, *26*, 4637−4646.
(10) Kang, X. H.; Wang, J.; Wu, H.; Aksay, I. A.; Liu, J.; Lin, Y. H. *Biosens. Bioelectron.* **2009**, *25*, 901−905.
(11) Zuo, X.; He, S.; Li, D.; Peng, Cheng.; Huang, Q.; Song, S.; Fan, C. *Langmuir* **2010**, *26*, 1936−1939.
(12) Huang, X.; Yin, Z. Y.; Wu, S. X.; Qi, X. Y.; He, Q. Y.; Zhang, Q. C.; Yan, Q. Y.; Boey, F.; Zhang, H. *Small* **2011**, *7*, 1876−1902.
(13) Guo, S. J.; Dong, S. J. *Chem. Soc. Rev.* **2011**, *40*, 2644−2672.
(14) Zhang, Y. W.; Liu, S.; Wang, L.; Qin, X. Y.; Tian, J. Q.; Lu, W. B.; Chang, G. H.; Sun, X. P. *RSC Adv.* **2012**, *2*, 538−545.
(15) Kumar, S. A.; Wang, S. F.; Yang, T. C. K.; Yeh, C. T. *Biosens. Bioelectron.* **2010**, *25*, 2592−2597.
(16) Ronkainen, N. J.; Halsall, H. B.; Heineman, W. R. *Chem. Soc. Rev.* **2010**, *39*, 1747−1763.
(17) Rahman, M. M.; Ahammad, A. J. S.; Jin, J. H.; Ahn, S. J.; Lee, J. J. *Sensor* **2010**, *10*, 4855−4886.
(18) Parra-Alfambra, A. M.; Casero, E.; Petit-Domínguez, M. D.; Barbadillo, M.; Pariente, F.; Vázquez, L.; Lorenzo, E. *Analyst* **2011**, *136*, 340−347.
(19) Gangadharan, R.; Anandan, V.; Zhang, A.; Drwiega, J. C.; Zhang, G. G. *Sens. Actuators B* **2011**, *160*, 991−998.
(20) Chen, Z. P.; Ren, W. C.; Gao, L. B.; Liu, B. L.; Pei, S. F.; Cheng, H. M. *Nat. Mater.* **2011**, *10*, 424−428.
(21) Cao, X. H.; Shi, Y. M.; Shi, W. H.; Lu, G.; Huang, X.; Yan, Q. Y.; Zhang, Q. C.; Zhang, H. *Small* **2011**, *7*, 3163−3168.
(22) Yong, Y. C.; Dong, X. C.; Chan-Park, M. B.; Song, H.; Chen, P. *ACS Nano* **2012**, *6*, 2394−2400.
(23) Maiyalagan, T.; Dong, X. C.; Chen, P.; Wang, X. *J. Mater. Chem.* **2012**, *22*, 5286−5290.
(24) Dong, X. C.; Wang, P.; Fang, W. J.; Su, C. Y.; Chen, Y. H.; Li, L. J.; Huang, W.; Chen, P. *Carbon* **2011**, *49*, 3672−3678.
(25) Dong, X. C.; Li, B.; Wei, A.; Cao, X. H.; Chan-Park, M. B.; Zhang, H.; Li, L. J.; Huang, W.; Chen, P. *Carbon* **2011**, *49*, 2944−2949.
(26) Huang, Y. X.; Dong, X. C.; Shi, Y. M.; Li, C. M.; Li, L. J.; Chen, P. *Nanoscale* **2010**, *2*, 1485−1488.
(27) Graf, D.; Molitor, F.; Ensslin, K.; Stampfer, C.; Jungen, A.; Hierold, C.; Wirtz, L. *Nano Lett.* **2007**, *7*, 238−242.
(28) Brownson, D. A. C.; Munro, L. J.; Kampouris, D. K.; Banks, C. E. *RSC Adv.* **2011**, *1*, 978−988.
(29) Zhu, J.; Chen, X.; Yang, W. S. *Sens. Actuators B* **2010**, *150*, 564−568.
(30) Ding, Y.; Wang, Y.; Su, L.; Bellagamba, M.; Zhang, H.; Lei, Y. *Biosens. Bioelectron.* **2010**, *26*, 542−548.
(31) Huang, K. J.; Jing, Q. S.; Wu, Z. W.; Wang, L.; Wei, C. Y. *Colloids Surf., B* **2011**, *88*, 310−314.
(32) Kim, Y. R.; Bong, S.; Kang, Y. J.; Yang, Y.; Mahajan, R. K.; Kim, J. S.; Kim, H. *Biosens. Bioelectron.* **2010**, *25*, 2366−2369.
(33) Cui, R. J.; Wang, X. Y.; Zhang, G. H.; Wang, C. *Sens. Actuators B* **2012**, *161*, 1139−1143.
(34) Zhou, M.; Zhai, Y.; Dong, X. J. *Anal. Chem.* **2009**, *81*, 5603−5613.